

Coherent radio emission from the electron beam sudden appearance

Krijn D. de Vries^{*a}, Masaki Fukushima^b, Romain Gaior^{cd}, Kael Hanson^e, Daisuke Ikeda^b, Yusuke Inome^f, Aya Ishihara^c, Takao Kuwabara^c, Keiichi Mase^c, John Matthews^g, Thomas Meures^e, Pavel Motloch^h, Izumi S. Ohta^f, Aongus O'Murchadha^e, Florian Partous^a, Matthew Relich^c, Hiroyuki Sagawa^b, Tatsunobu Shibataⁱ, Bokkyun Shin^j, Gordon Thomson^g, Shunsuke Ueyama^c, Tokonatsu Yamamoto^f, Shigeru Yoshida^c

^aVrije Universiteit Brussel, Dienst ELEM, IIHE, Pleinlaan 2, 1050, Brussel, Belgium

^bICRR, University of Tokyo, 5-1-5 Kashiwanoha, Kashiwa, Chiba 277-8522, Japan

^cDepartment of Physics, Chiba University, Yayoi-cho 1-33, Inage-ku, Chiba 263-8522, Japan

^dLaboratoire de Physique Nucléaire et de Hautes Energies (LPNHE), Universités Paris 6 et Paris 7, CNRS-IN2P3, France

^eDept. of Physics and Wisconsin IceCube Particle Astrophysics Center, University of Wisconsin, Madison, WI 53706, USA

^fFaculty of Science and Engineering, Konan University, Kobe 658-8501, Japan

^gPhysics And Astronomy, University of Utah, 201 South, Salt Lake City, UT 84112, U.S.

^hKavli Institute for Cosmological Physics & Department of Physics, University of Chicago, Chicago, IL 60637, USA

ⁱHigh Energy Accelerator Research Organization (KEK), 2-4 Shirakata-Shirane, Tokai-mura, Naka-gun, Ibaraki, 319-1195, Japan

^jOsaka City University, Osaka 558-8585, Japan

E-mail: krijndevries@gmail.com

We report on radio frequency measurements of the electron beam sudden appearance signal from the Telescope Array Electron Light Source (TA-ELS). The TA-ELS is constructed to calibrate the Telescope Array fluorescence telescope, and as such it can be used to mimic a cosmic-ray or neutrino induced particle cascade. This makes the TA-ELS the perfect facility to study new detection techniques such as the radio detection method. We report on the data obtained by four independent radio detection set-ups. Originally searching for either the direct Askaryan radio emission, or a radar echo from the induced plasma, all these experiments measured a very strong transient signal when the beam exits the accelerator. Due to the different scope of the individual experiments, we have detected the beam sudden appearance signal at different frequencies, ranging between 50 MHz and 12.5 GHz. The direct application in nature for this signal is found in cosmic-ray or neutrino induced particle cascades traversing through different media, such as air, ice, and rock. These measurements are compared to the theoretical predictions for this signal, where it follows that theory and experiment match very well over the full spectrum.

35th International Cosmic Ray Conference -ICRC2017-

10-20 July, 2017

Bexco, Busan, Korea

*Speaker.

1. Introduction

At the highest energies, the cosmic-ray particle flux drops rapidly [1, 2, 3]. Therefore, to probe these particles, a very large detection volume is needed. Due to its long attenuation length, in combination with the cost-efficient detectors, the radio signal is extremely suited to probe this flux. To test the radio detection technique, in recent years several beam test experiments have been performed [4, 5, 6, 7, 8, 9]. One of the main backgrounds for several of these experiments was given by transition radiation, or as will be outlined in this work the beam sudden appearance emission.

We report on the measurement of coherent radio emission from the electron beam sudden appearance at the Telescope Array Electron Light Source (TA-ELS) facility [10]. This signal was detected by four independent experiments searching for either a direct radio signal from the high-energy electron beam which was directed in to the air or ice [11, 12], or the indirect radar scatter from the plasma induced by the beam [13, 14]. Due to the different nature of these experiments, the electron beam sudden appearance signal was probed over a wide frequency range from 50 MHz up to 12.5 GHz. We show that this signal can be described as an extreme form of coherent transition radiation, and resembles the particle distributions in the beam.

The direct application of this signal can be two-fold. Since the observed sudden appearance radiation gives a strong transient signal which resembles the particle distributions in the particle beam, it can be used for either triggering purposes to denote the time at which the beam exits the accelerator, or if detected in more detail, as a beam monitor signal. The in-nature application of this signal is found in cosmic-ray or neutrino induced particle cascades traversing different media such as air, ice, and rock [15, 16].

2. The Telescope Array Electron Light Source facility

The Telescope Array is the largest ultra-high-energy cosmic-ray observatory in the Northern hemisphere [17]. Cosmic ray air showers are detected by either the particle footprint or the fluorescence light emitted when the particle cascade traversed the air. For the absolute calibration of the fluorescence detectors, the TA-ELS has been constructed. The TA-ELS is located 100 m away from one of the fluorescence telescopes. To mimic a cosmic-ray induced particle cascade, a high-energy electron beam is directed in to the air with a repetition rate of 0.5 Hz. This beam typically consists out of $10^8 - 10^9$ electrons with an average energy of roughly 40 MeV per electron. Once the beam has left the beam exit window, it will reach a height of roughly 130 m in air. Consequently the detected fluorescence light is cross-calibrated against the total energy in the beam, where the latter is determined by using pick-up coils and a Faraday Cup. The total accuracy is estimated to roughly 3 %.

Since the total energy in the beam is ~ 40 PeV, the TA-ELS facility provides the ideal environment to test new detection techniques to probe such high-energy particle cascades. For these experiments typically a high beam intensity is favored, where the output charge from the TA-ELS is limited due to radiation safety. Therefore, the beam bunch length which in its standard configuration is roughly $1 \mu\text{s}$, was altered to either 20 ns by using the original TA-ELS variable pulser or to 2 ns by using a fast pulser.

The beam charge profile is shown in the left figure of Fig. 1. The beam is constructed out of multiple sub-bunches with a 2.856 GHz repetition rate. The right figure of Fig. 1 shows the lateral particle distribution of the beam at 1 m from the beam exit window as estimated from GEANT4 simulations [18].

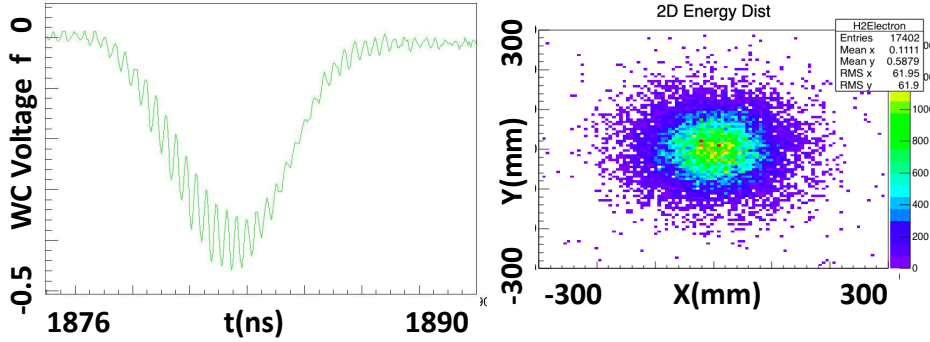


Figure 1: The electron beam particle distributions for the roughly 2 ns wide beam bunch. The left figure shows the Wall Current voltage as function of time in ns. The beam is constructed out of several sub-bunches with a 2.856 GHz repetition rate. The right figure shows the lateral particle spread obtained from GEANT4 simulations at 1 m from the beam exit point. The spread is found to be of the order of several centimeters.

3. Radio detection experiments

In this section we give an outline of the different radio detector set-ups used for this analysis. Furthermore, a brief outline of the initial goal of the experiment is presented. The presentation will be done in order of the frequency band at which the experiments operated.

3.1 50 MHz experiment

The basic idea of this experiment is to search for the in-air radar echo from the electron beam induced by TA-ELS [19]. The transmitter and receiver are installed at a distance of 140 m from the ELS (see Fig. 2, top left). A wide-band receiver system was used consisting of a log-periodic antenna of 4 meters length, sensitive in the 50-1300 MHz band and with a directional gain of 10 dBi (Creative Design; CLP5130-1D). The antennas were installed horizontally to the beam exit. The signal from the antenna passes through 20 meters of LMR-400 coaxial cable into the data acquisition (DAQ) system, which consists of a band pass filter, pre-amplifier and a digitizer. An FM cut filter (stop 88-108 MHz) is employed along with low pass (< 100 MHz) and highpass (> 25 MHz) filters. The signal is consequently lead to a wideband pre-amplifier (Anritsu;MH648A) with a variable gain up to 30 dB. Finally, the signal is digitized by the Software-Defined Radio system (Ettus; USRP) with a quadrature detection method of 25 MHz, 14 bits sampling. The total acceptable band range of this receiver is from 50 MHz to 66 MHz. The receiver system is calibrated by using a network analyzer at the Microwave Energy Transmission LABORatory (METLAB) [21] at Kyoto university.

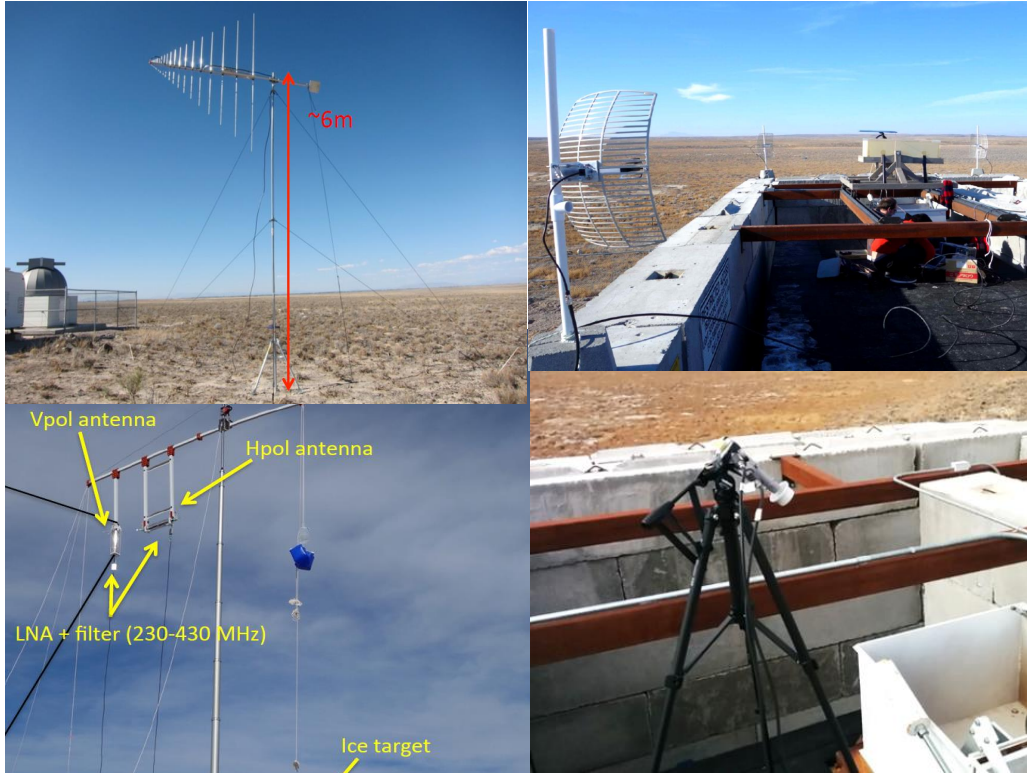


Figure 2: The four different experimental set-ups used for this analysis. The different antenna setups are given by a log-periodic antenna set-up (50 MHz ; top left), the ARA antenna set-up (230-430 MHz; bottom left), the Wifi-bow antenna set-up (1.4-3 GHz ; top right), and the feed-horn set-up (12.5 GHz ; bottom right).

3.2 230-430 MHz experiment

The ARACalTA experiment was performed in January 2015, using the TA ELS electron beam to characterize the Askaryan effect in ice as well as to confirm the detector simulation and calibration [11]. The radio signal is collected by the same antennas as the ones used for the ARA experiment [22]. Besides the runs operated with the ice target, ARACalTA also acquired data of the radio background produced when no target was present, i.e. when the beam was shot directly into the air. Only these runs will be used for the analysis presented in this work.

The antennas were located at a perpendicular distance of 7.3 m from the beam axis, and the bunch length for this experiment was decreased by a fast pulser to around 2 ns. For the charge measurement, in addition to the Faraday Cup and the pickup coil, a Wall Current Monitor was setup to permit the measurement of the charge waveform without absorbing the charge unlike the Faraday Cup. The antennas are set up orthogonally to measure two polarizations, and have a dipole like radiation pattern (see Fig. 2, bottom left). Each of them is directly followed by a bandpass filter which selects the frequencies between 230-430 MHz, after which a low noise amplifier boosts the signal by about 40 dB. The signal is transported over 40 meter LMR-400 coaxial cable and recorded with a fast oscilloscope at 10 GSa/s. A dedicated run using a calibrated antenna as a radiation source served as a verification for the simulation of the full signal chain. The uncertainties on the power

measurement were estimated using the obtained data, and were found to be less than 15% [11].

3.3 1.4-3 GHz experiment

The 1.4 GHz - 1.9 GHz measurements were obtained as a side experiment of the ARAlTA experiment. Hence, the beam configurations were similar. This experiment investigated the radar detection technique to probe high-energy particle cascades in ice [14]. The receiver antenna used for the analysis presented in this work was located at 2.83 m horizontally from the beam exit. The data was obtained using a broadband 1.4-3 GHz Hyperlink HG2420, high gain 24 dBi, WiFi bow antenna (see Fig. 2, top right). The data was transferred over a 30 m LMR-400 cable after which it was amplified (+15 dB ZX60-6013) and read out by a 10 GSa/S Agilent MSO9254 scope.

3.4 12.5 GHz experiment

The intensity of the 12.5 GHz microwave radiation from the electron-beam exit was measured on the roof of the ELS building. This measurement aimed to probe the expected Molecular Bremsstrahlung Radiation from air-showers caused by Ultra-High-Energy Cosmic Rays [20]. A feed-horn-receiver unit with a bandwidth between 12.25 - 12.75 GHz (Nippon Antenna FOC-ASJ5) is fixed near the beam exit (see Fig. 2, bottom right). The distance from the beam exit is 1.64 m and the emission angle between line of the sight of feed-horn and electron beam is 55 degrees. The receiver has two channels to measure the vertical and horizontal polarizations. The microwave signal from the feed-horn antenna is converted down to 0.95 - 1.45 GHz by a local oscillator. The signal from the down-converter is consequently boosted by an amplifier and transferred to a power detector through a 6 m LMR-400 co-axial cable. The total gain of the detector chain is 75.6 dB. The power detector converts the signal amplitude to a voltage which is measured by a digital oscilloscope and stored.

4. The electron beam sudden appearance signal

As indicated, all four experiments detected an unexpected strong transient signal when the electron beam left the accelerator. In this section we discuss the theoretical explanation for this signal, which was recently outlined in [15, 16, 23, 24]. In these works, this signal was applied to the in-nature situation of a high-energy cosmic-ray or neutrino induced particle cascade traversing between different media such as air and ice, or rock. Since no such signal has been detected in nature so-far, the experimental results obtained in this work allow us to test these model predictions in detail for the first time.

Where in [16], a microscopic approach was used and the radio signal was obtained from a superposition of the emission of the individual electrons, in [15] a macroscopic description was presented which will be outlined in the following. While the electron beam is traversing inside the TA-ELS, it is hidden for the observer. Note that hidden means that the radiation is absorbed by the accelerator tube and re-emitted outside the sensitive, coherent, frequency band. Hence, only the coherent emission is considered in the following. In this situation, the vector potential vanishes while the beam traverses inside the TA-ELS, and becomes 'suddenly' visible when the beam exits the accelerator. Since the field is obtained from the derivative of the potential, for a single electron this leads to an instantaneous emission. Nevertheless, for coherent emission this

does not pose a problem, since a cut-off scale is defined by the dimensions of the beam bunch structure. Consequently the electric field for an observer located at \vec{x} at a time t is obtained as [15],

$$\vec{E}_{sa}(t, \vec{x}) = \lim_{\varepsilon \rightarrow 0} \int d^2r \frac{e d N_e(t_r) w(\vec{r}, h)}{4\pi \varepsilon_0 c |\mathcal{D}|_{t_r+\varepsilon}^2} \hat{p} \Big|_{h=c(t_r-t_b)}. \quad (4.1)$$

Here \vec{r} denotes the lateral position of the emission point in the beam, d gives the impact distance, $N_e(t_r)$, denotes the total number of charges at the emission time t_r , and $w(r, h)$ gives the longitudinal and lateral particle distribution at the time t_r . The retarded four-distance is given by $\mathcal{D} = R(1 - n\beta \cos(\theta))$, where R is the distance from the emission point to the observer, n , the refractive index of air, $\beta = v/c$, the charge velocity, and θ denotes the opening angle between the line of sight to the emission point and the direction of motion of the charge. The geometry is shown in Fig. 3. From this expression, it immediately follows that the expected signal resembles the charge distributions $N_e(t_r)$, and $w(r, h)$, for a fixed geometry.

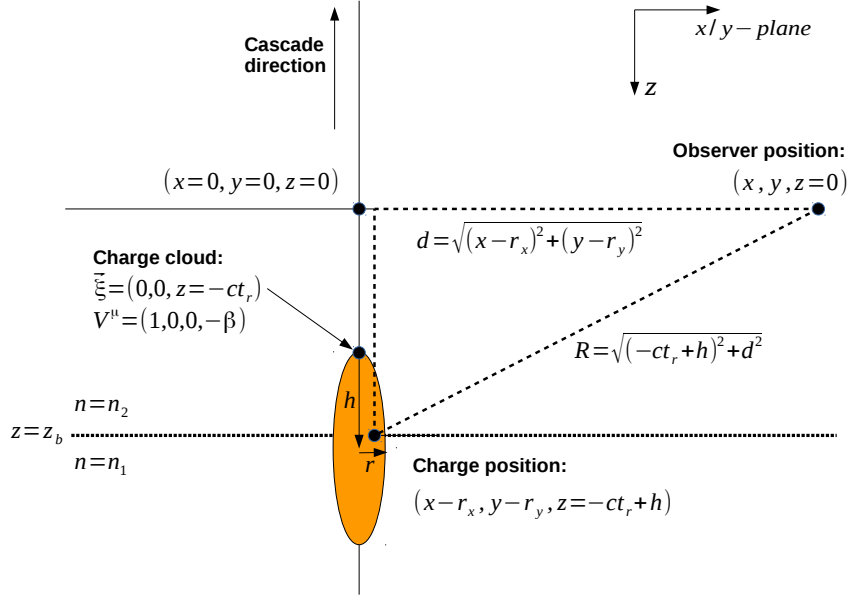


Figure 3: The geometry used to calculate the radiation emitted from a charge cloud crossing a boundary at $z = z_b$. The observer is positioned at an impact parameter $d = \sqrt{(x - r_x)^2 + (y - r_y)^2}$. Figure and caption taken from [15].

5. Simulation and Results

In Fig. 4, we show the signal that is expected at a horizontal distance of 1 m from the beam exit. This signal is simulated using the microscopic formalism described in [16], using a GEANT4 simulation [18] for the particle propagation. The simulated power density is given by the full black line in Fig. 4. To understand this profile, we need to consider the different length scales of the particle distributions. The longest length scale is given by the beam bunch length which for this

simulation was taken from the roughly 2 ns beam width configuration. This leads to strong coherence up to a few hundreds of MHz, after which the signal strength drops rapidly. Consequently, at 2.856 GHz, we see a coherence over the sub-bunch structure, after which the signal drops again, but still shows coherence over the lateral particle distributions which are of the order of several centimeters. At the highest frequencies, the signal magnitude drops rapidly.

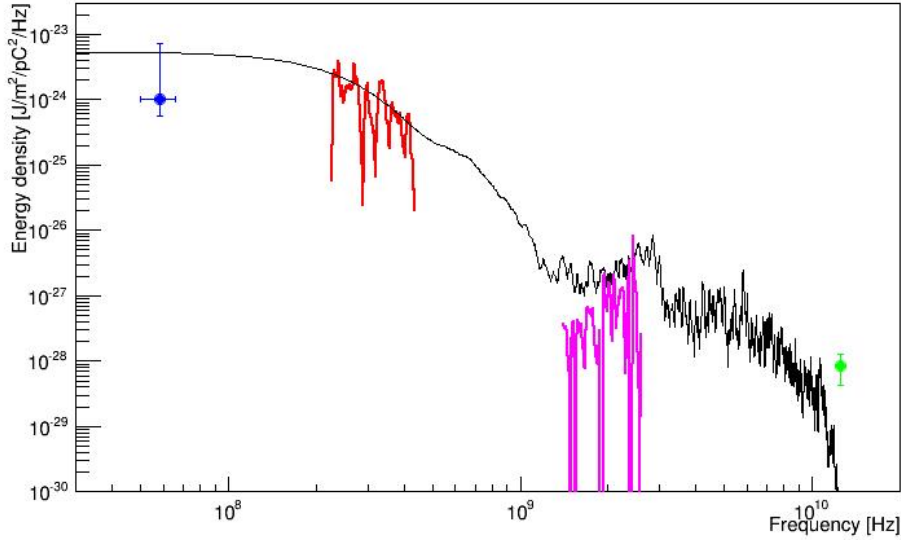


Figure 4: The simulated power density for a 2 ns bunch width. Furthermore, we show the obtained experimental data (50 MHz: blue dot, 230-430 MHz: red line, 1.4-3 GHz: purple line, 12.5 GHz: green dot).

In Fig. 4, we also plot the data obtained by the different experiments. To have a quantitative comparison, each experiment should be compared to a dedicated simulation due to its different geometry. Even-though the 50 MHz and 12.5 GHz experiments were performed using a 20 ns bunch width, at their corresponding frequencies the simulation does not differ from the simulation for the 2 ns bunch width. Therefore, assuming an R^{-2} far-field scaling of the signal strength, we can make a qualitative comparison between data and simulation. It follows that already in this qualitative comparison the overall signal strength, which drops over many orders of magnitude shifting to higher frequencies, agrees very well with the simulated signal. Furthermore, the effects of the different beam-bunch structures are observed from the data.

6. Summary

We reported on the measurement of the electron beam sudden appearance signal, detected at the Telescope Array Electron Light Source facility. Four different radio detection experiments all measured an unexpected very strong transient signal from the electron beam appearing from the accelerator. It is shown that this signal can be described as an extreme form of coherent transition radiation. A qualitative comparison between the obtained data and the simulated sudden appearance signal is given. It follows that the signal strength, which drops over many orders of magnitude

while shifting to higher frequencies, agrees very well with simulations. Furthermore, the observed data directly reflects the different length scales of the electron beam.

Acknowledgments

The authors would like to thank the Telescope Array collaboration for the use of the TA-ELS facility and their indispensable assistance in obtaining the experimental results presented in these proceedings.

References

- [1] Peter Tinyakov, for the Telescope Array Collaboration, *Nuclear Instruments and Methods in Physics Research A* **742**,(2014), 29-34
- [2] The Pierre Auger Collaboration, *ApJ* **804** (2015) 1
- [3] IceCube Collaboration, *Science* **342** (2013) 1242856
- [4] D. Saltzberg et al., *Phys. Rev. Lett.* **86** (2001) 2802
- [5] P. W. Gorham et al., *Phys. Rev. E* **62** (2000) 8590
- [6] P. W. Gorham et al., *Phys. Rev. D* **72** (2005) 023002
- [7] P. W. Gorham et al., *Phys. Rev. Lett.* **99** (2007) 171101
- [8] P. Miocinovic et al., *Phys. Rev. D* **74** (2006) 043002
- [9] K. Belov et al., *Phys. Rev. Lett.* **116** (2016) 141103
- [10] T. Shibata et al., *Nucl. Instr. Meth. A* **597** (2009) 61-66
- [11] K. Mase et al., [PoS \(ICRC2015\) 1136](#) (2016)
- [12] I.S. Ohta et al, *Nucl. Instrum. Meth. A* **810** (2016) 44-50
- [13] D. IKEDA et al., *Proceedings of the 33rd ICRC* (2013) 360
- [14] K.D. de Vries et al., [PoS \(ICRC2015\) 1168](#) (2015)
- [15] K.D. de Vries et al., *Astropart. Phys.* **74** (2016) 96-104
- [16] P. Motloch et al., *Phys. Rev. D* **94** (2016) 049905
- [17] H. Kawai, et al., *Nucl. Phys. Proc, suppl* **175-176** (2008) 221-226
- [18] S. Agostinelli et al., *Nucl. Instrum. Meth. A* **506** (2003) 250
- [19] P.W. Gorham, *Astropart. Phys.* **15** (2001) 177-202
- [20] P. W. Gorham et al., *Phys. Rev. D* **78** (2008) 032007
- [21] <http://www.rish.kyoto-u.ac.jp/DCRP/METLAB.html>
- [22] P. Allison et al., *Astropart. Phys.* **35** (2012) 457-477
- [23] B. Revenu, V. Marin, *arXiv:1211.3305*
- [24] K.D. de Vries et al., *EPJ Web Conf.* **135** (2017) 05001